35. Structure and Highly Stereoselective Formation of 1:2 Metal-to-Ligand Complexes with the Triamine 2,6-Bis(pyrrolidin-2-yl)pyridine. *meso*-[2,6-Bis(pyrrolidin-2-yl)pyridine]nickel(II) (*meso*-$[Ni(bpp)_2]^{2+}$), a Metal Complex with S_4 Symmetry[1])

by **Klaus Bernauer***, **François Gretillat**, **Helen Stoeckli-Evans**, and **Ruth Warmuth**

Institut de chimie, Université de Neuchâtel, 51, av. de Bellevaux, CH-2000 Neuchâtel

(1.X.92)

The X-Ray structures of the 1:1 copper(II) complexes with racemic and optically active (+)-(*R*,*R*)-(2,6-bis(pyrrolidin-2-yl)pyridine ((+)-bpp; (+)-**I**) were determined. Whereas the perchlorate **1** of the racemic complex contains the monomeric units with perfect C_2 symmetry, the sulfate of the optically active compound crystallizes as a coordination polymer composed of sequences of three different five-coordinate units linked by sulfate bridges around a threefold screw axis (see **2**). Formation of the 1:2 complexes of nickel(II) with (±)-bpp is shown to be highly stereoselective. Acidimetric titrations and CD measurements indicate that the equilibrium mixture contains 99% of the *meso*-complex **3** belonging to the point group S_4 and only 0.5% of each enantiomer of the C_2-symmetric optically active forms. The S_4 symmetry of *meso*-[Ni{(+)-bpp}{(−)-bpp}]$(ClO_4)_2$ (**3**) was confirmed by X-ray analysis. The formation of binary complexes of cobalt(II), zinc(II), and cadmium(II) with (±)-bpp shows an excess of 28, 34, and 8%, respectively, of the *meso*-form over the statistical amount. CD and UV/VIS measurement show a pH-dependent high spin/low spin equilibrium between the octahedral $[Ni(bpp)(H_2O)_3]^{2+}$ and the square-planar $[Ni(bpp)OH]^+$ in aqueous solution.

1. Introduction. – The synthesis of the (*R*,*R*)-, (*S*,*S*)-, and (*R*,*S*)-isomers of the triamine 2,6-bis(pyrrolidin-2-yl)pyridine (**I**) and the 1:1 complex formation of these ligands with Cu^{2+} were reported in a preceding paper [2]. This ligand system was designed for its peripheral coordination mode and the rigid arrangement of the chiral centers in the corresponding coordination compounds. This rigid structure should be conserved in solu-

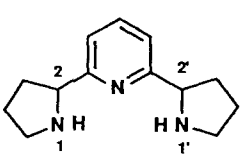

I bpp

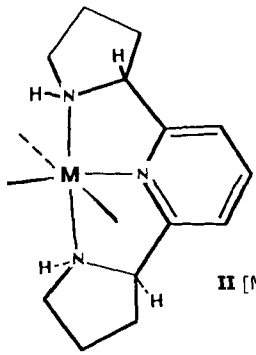

II [M{(*R*,*R*)-bpp}]

[1]) Part XVI of 'Stereoselectivity in Reactions of Metal Complexes'. For part XV, see [1].

tion reactions leading to binary as well as mixed ligand complexes and, therefore, stereoselective effects observed in these reactions should be easier to explain than for systems containing more flexible ligands. The two optically active isomers would be expected to coordinate stereospecifically in C_2-symmetric, S-shaped arrangements allowing only the (1*S*,1*S*′,2*S*,2*S*′)- and the (1*R*,1*R*′,2*R*,2*R*′)-configurations (see **II**).

In the formation of binary complexes with bpp, two clearly distinct geometries are possible, depending on whether the two bpp ligands show the same or the opposite absolute configuration. If one looks down the symmetry axis of these two geometric arrangements (see *Fig. 1* for a schematic representation), pairs of the five-membered pyrrolidine rings are oriented into the (clockwise numbered) quadrants II and IV for $[M\{(R,R)\text{-bpp}\}_2]^{2+}$ and I and III for $[M\{(S,S)\text{-bpp}\}_2]^{2+}$, respectively. In the *meso*-complex with S_4 symmetry, on the other hand, each five-membered ring points into a different quadrant. Thus, the nonbonding interactions between the two ligand molecules should be more important in the optically active complexes than in the *meso*-compound, and in the equilibrium mixture, the latter should be favoured over the former.

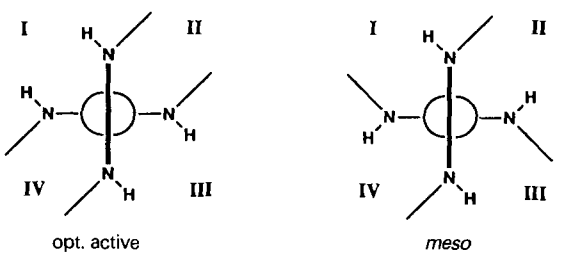

Fig. 1. *Schematic representation of optically active* $[M\{(R,R)\text{-bpp}\}_2]^{2+}$ *and* meso-$[M\{(R,R)\text{-bpp}\}\{(S,S)\text{-bpp}\}]^{2+}$ *viewed down the symmetry axis*

2. Equilibrium Measurements. – To detect stereoselectivity in the Ni/(±)-bpp system, circular dichroism (CD) measurements were first applied using the technique of continuous variation of enantiomers previously described [3]. From the results show in *Fig. 2*, nearly quantitative stereoselectivity in favour of the *meso*-complex can be deduced. Unfortunately, the method, which is favourable in the case of weak stereoselectivity, does not allow the precise determination of the isomer ratio if one of the two forms, *meso* or optically active, is strongly preferred with respect to the other[2]).

On the other hand, a high stability of the *meso*-compound relative to the optically active forms can be determined easily and precisely by comparison of acidimetric titrations of 1:2 metal to ligand mixtures obtained either with the optically active or the racemic ligand [4]. In the system Ni/(±)-bpp, the high stereoselectivity in favour of the *meso*-compound is confirmed by an important separation of the two titration curves starting immediately after the addition of the first equiv. of NaOH and reaching 0.80 pH units at 1.5 equiv. (*Fig. 3*).

---

[2]) From the equilibrium constants given in *Table 1*, it can be calculated that the condition of complete formation of the binary species is not fulfilled under the conditions given in *Fig. 2*. Disregarding a possible influence of *Tris* buffer, the amount of 1:1 complex in the equilibrium mixture is *ca.* 5% with the optically active ligand, whereas it is present at less than 0.2% with the racemic ligand.

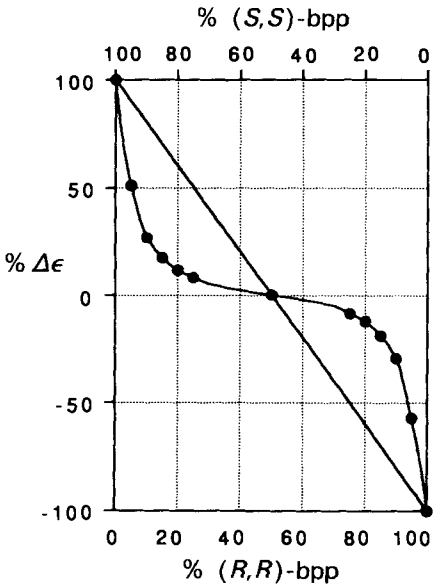

Fig. 2. *Relative circular-dichroism intensity* ($\lambda = 555$ nm) *for continuous variation of enantiomers.* $[Ni^{2+}]_{tot} = 1.5 \cdot 10^{-3}$ M; $[R]_{tot} + [S]_{tot} = 2.25 \cdot 10^{-2}$ M; pH 9.5 (0.025M *Tris*-HCl).

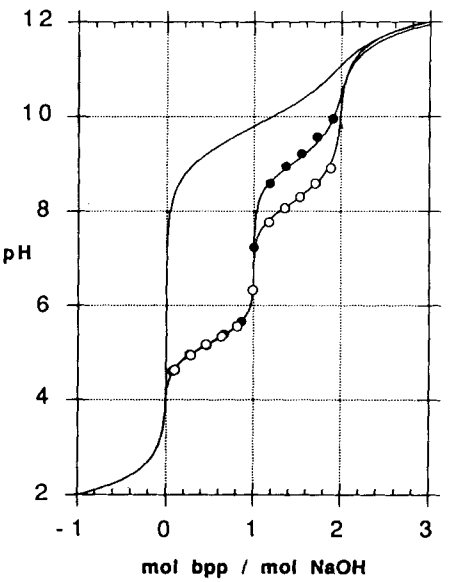

Fig. 3. *Potentiometric titration curves for Ni^{2+}/bpp 1:2 mixtures.* a) $[HCl]_{tot} = 2.3 \cdot 10^{-2}$ M; $[Ni^{2+}]_{tot} = 5.34 \cdot 10^{-3}$ M; [(+)- and (−)-bpp]$_{tot} = 1.07 \cdot 10^{-2}$ M; b) $[Ni^{2+}]_{tot} = 4.77 \cdot 10^{-3}$ M; [(−)-bpp]$_{tot} = 9.54 \cdot 10^{-3}$ M. Temp. 25°; $\mu = 0.12$ (KNO_3). Open circles, racemic ligand; full circles, optically active ligand; lines, calculated curves obtained from mean values of the stability constants given in *Table 1.*

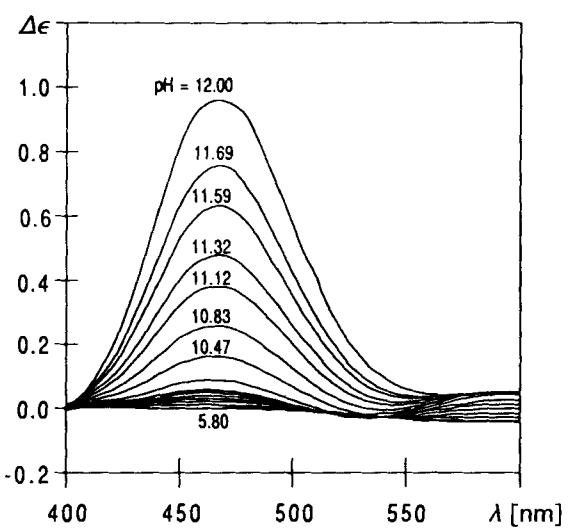

Fig. 4. *CD Spectra of a Ni^{2+}/(−)-bpp 1:2 mixtures at various pH.* $[Ni^{2+}] = 3.14 \cdot 10^{-3}$ M; [(−)-bpp] $= 6.31 \cdot 10^{-3}$ M.

At pH > 10, a net colour change of the solutions from light violet to bright yellow is observed due to the appearence of an intense absorption band at 21 700 cm^{-1}, typical for low-spin square-planar nickel(II) complexes [5]. To this band corresponds a CD band at λ 468 nm for the optically active compound (*Fig. 4*). As the yellow species appears at lower pH in the titration of the 1:2 mixture containing the optically active ligand, which, compared to the racemic ligand, forms the less stable binary complex, the change from the high-spin octahedral to the low-spin square-planar species can be explained by the substitution of one ligand molecule by an OH^- ion according to *Eqn. 1*. This is confirmed

$$[Ni(bpp)_2]^+ + OH^- \rightleftharpoons [Ni(bpp)OH]^+ + bpp \quad (1)$$

by the titration of a 1:1 mixture containing the optically active ligand. For such a system, the 1:2 species is almost nonexistent. The *Equilibrium 1* offers an interesting example of stereoselectivity directly visible by the naked eye: solutions of 1:2 mixtures of Ni^{2+} with either enantiomer of bpp at pH 12 are deep yellow, but when equal volumes of these solutions are mixed, the colour immediately turnes to pale violet. On the other hand, the pH-dependent *Equilibrium 2* between the aqua- and the hydroxyspecies represents an

$$\underset{\text{octahedral}}{[Ni(bpp)(H_2O)_3]^{2+}} + OH^- \rightleftharpoons \underset{\text{square-planar}}{[Ni(bpp)OH]^+} + 3\,H_2O \quad (2)$$

elegant demonstration of the higher ligand-field strength of the OH^- ion compared to H_2O in Ni^{II} complexes.

The equilibrium constants obtained from potentiometric titrations for Co^{2+}, Ni^{2+}, Cu^{2+}, Zn^{2+}, and Cd^{2+} are reproduced in *Table 1*. From these constants, it can be calculated that, for all the metal ions showing 1:2 coordination with bpp, the *meso*-complex is distinctly more stable and present at 78, 99, 80, and 58% for Co^{2+}, Ni^{2+}, Zn^{2+}, and Cd^{2+}, respectively.

3. Structures. – X-Ray crystal structures were obtained for three complexes: $[Cu\{(\pm)\text{-bpp}\}H_2O](ClO_4)_2 \cdot 2\,H_2O$ (**1**), $[Cu\{(+)\text{-bpp}\}]_3(SO_4)_3 \cdot 2\,H_2O \cdot$ [(−)-di-*O*,*O*′-(4-toluoyl)-L-tartaric acid] (**2**), and $[Ni\{(+)\text{-bpp}\}\{(-)\text{-bpp}\}](ClO_4)_2 \cdot H_2O$ (**3**).

$[Cu\{(\pm)\text{-bpp}\}H_2O](ClO_4)_2$ (**1**). The structure of the 1:1 complex of copper(II) and (±)-bpp is shown in *Fig. 5*. Selected bond lengths and angles are given in *Table 2*. The cation has crystallographic C_2 symmetry and the coordination of the copper atom is square-planar. The chelate ring Cu(1), N(1), C(1), C(6), N(2) is planar within 0.004(1) Å. The five-membered pyrrolidine ring has an envelope conformation with the atom C(8) displaced by 0.61(1) Å from the best plane through the atoms N(2), C(6), C(7), and C(9). This latter plane is inclined by 52.8(2) ° to the plane of the chelate ring.

$[Cu\{(+)\text{-bpp}\}]_3(SO_4)_3 \cdot 2\,H_2O \cdot \{(-)$-di-O,O′-(4-toluoyl)-L-tartaric Acid$]$ (**2**). The complex of copper(II) and (+)-bpp shown in *Fig. 6* was studied to determine the absolute configuration of the optically active ligand. The complex crystallized as a coordination polymer with a basic unit of three different five-cooridnate Cu^{II} units linked by sulfate bridges around a local three-fold screw axis, which is parallel to the *a* axis of the unit cell. Selected bond lengths and bond angles are given in *Table 2*. The crystal was rather small and did not diffract significantly beyond 35° in 2 θ. It was not possible to refine all the non-H-atoms anisotropically, hence the accurracy in bond length and angles is not very

Table 1. *Protonation*[a]) *and Complex-Formation Constants*[b]) *of the System* M^{2+}/L. L = 2,6-Bis(pyrrolidin-2-yl)pyridine. T 25°; μ = 0.12 (KNO_3).

Ion M	K_{ML}	$K_{rac\text{-}ML_2}$	$K_{meso\text{-}ML_2}$	K_{MLOH}	$K_{ML(OH)_2}$	S[c])	% *meso*-complex	log K − log2	$\Delta\Delta G - RT\ln 2$[d])
Co^{2+}	9.10(2)	4.35(2)	5.21(3)	9.77(3)	–	3.6	78	0.56	3.19
Ni^{2+}	11.33(4)	3.94(3)	6.23(2)	11.75(10)	–	98	99	1.99	11.33
Cu^{2+}	16.80	–		8.49	–	–	–	–	–
Zn^{2+}	9.06(4)	3.54(6)	4.57(6)	9.08(2)	10.87(3)	5.29	84	0.72	4.12
Cd^{2+}	8.02(2)	5.70(5)	6 15(3)	–	–	1.4	58	0.14	0.80

[a]) $-\log K_1 = 9.40$; $-\log K_2 = 10.20$.

[b]) All constants are given as log K. $K_{meso\text{-}ML_2}$ represents the true stability constant of the mixed species. K_{MLOH} and $K_{ML(OH)_2}$ are defined as the − log of the stepwise acid dissociation constants. Errors in the last digits are given in parentheses.

[c]) Defined as $K_{meso}/2K_{rac}$.

[d]) In kJ mol^{-1}.

Table 2. *Selected Bond Lengths* [Å] *and Bond Angles* [°] *of Copper(II) Complexes with bpp.* Arbitrary numbering.

	[Cu{(±)-bpp}H_2O]$(ClO_4)_2 \cdot 2H_2O$ (**1**)	[Cu{(+)-bpp}]$_3(SO_4)_3 \cdot 2\,H_2O \cdot$(−)-di-*O,O′*-(4-toluoyl)-L-tartaric acid] (**2**)		
		cation 1	cation 2	cation 3
Cu–N(1)	1.912(4)	1.912(18)	1.908(17)	1.937(21)
Cu–N(2)	2.023(2)	1.984(18)	2.004(17)	2.027(18)
Cu–N(3)		2.004(18)	2.071(17)	2.041(19)
Cu–O(W1)	1.919(4)			
Cu–O(1)		1.948(15), S(3)	1.944(16), S(1)	1.924(17), S(2)
Cu–O(3)		2.303(15), S(1)	2.321(16), S(2)	2.396(16), S(3)
N(1)–Cu–N(2)	83.48(9)	81.7(8)	81.6(7)	82.5(8)
N(1)–Cu–N(3)		84.6(8)	83.5(7)	82.4(8)
N(1)–Cu–O(W1)	180.0			
N(1)–Cu–O(1)		169.8(8)	176.8(8)	175.7(8)
N(1)–Cu–O(3)		96.9(7)	90.6(7)	91.8(7)
O(1)–Cu–O(3)		93.1(6)	86.7(6)	92.5(6)

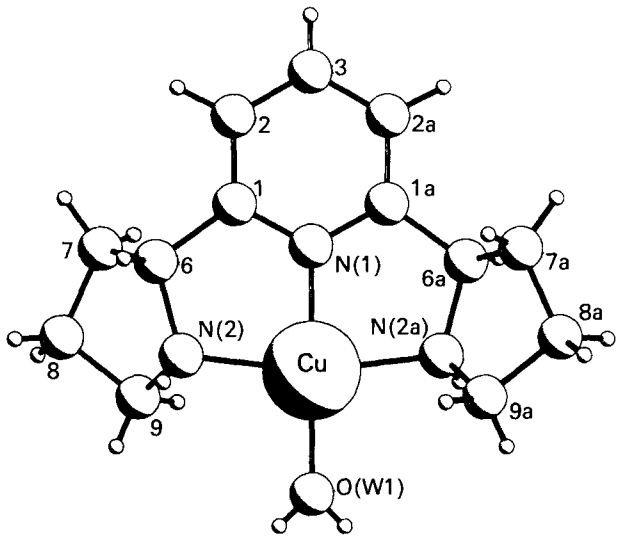

Fig. 5. *X-Ray crystal structure of* $[Cu\{(\pm)\text{-}bpp\}H_2O](ClO_4)_2 \cdot 2H_2O$ (**1**). The complex with the (*R*,*R*)-isomer of the ligand is represented. Arbitrary numbering.

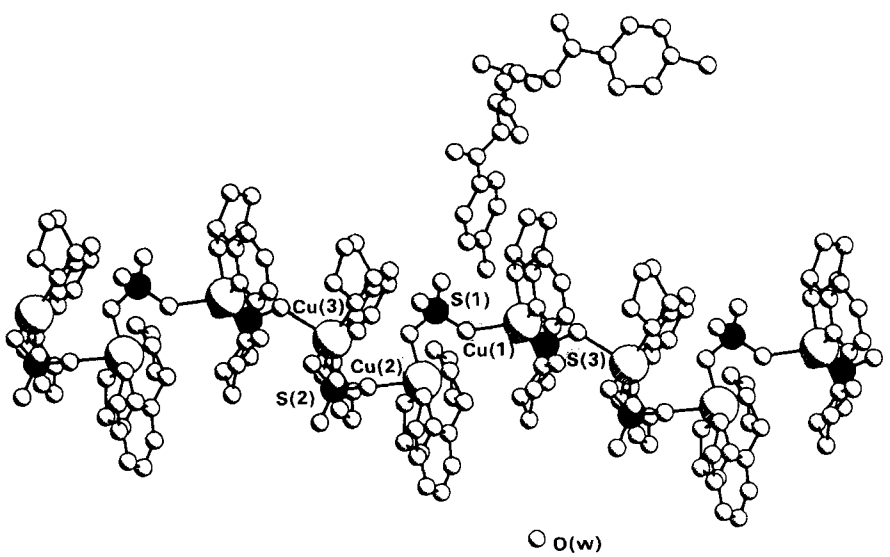

Fig. 6. *X-Ray crystal structure of* $\{[Cu\{(+)\text{-}bpp\}]_3(SO_4)_3 \cdot 2H_2O \cdot [(-)\text{-}di\text{-}O,O'\text{-}(4\text{-}toluoyl)\text{-}L\text{-}tartaric\ acid]\}_n$ (**2**). Arbitrary numbering.

high. The copper coordination in all three cations is square pyramidal, the pyramidal position being occupied by a bridging sulfate O-atom (mean Cu···O distance 2.340 Å).

In cations 1 and 3, the Cu-atom is displayed by −0.189 and 0.127 Å, respectively, from the best plane through atoms N(1), N(2), N(3), and the coordinated sulfate O-atom. In cation 2, the square plane N_3O is folded about the N(2)···N(3) axis with the Cu-atom

displaced in the direction of atoms N(1) and O(11). The pyrrolidine rings have envelope conformations, except that involving atom N(3) in cation 1 which has a half-chair conformation.

The crystal contains one molecule of (−)-di-*O*,*O*′-(4-toluoyl)-L-tartaric acid for each basic unit of three Cu-ions (only one molecule is represented in *Fig. 6*). The presence of these molecules allows the attribution of the absolute configuration of the ligand and the sense of helicity of the coordination polymer. By comparison of the configuration of the two asymmetric ligand C-atoms relative to the configuration of the (−)-di-*O*,*O*′-(4-toluoyl)-L-tartaric acid, it can be concluded that (+)-bpp ((+) at 589 nm) shows *(R,R)*-configuration and that for this enantiomer, the sense of rotation of the polymer around the threefold screw axis is counterclockwise.

[Ni{(+)-bpp}{(−)-bpp}](ClO$_4$)$_2$·H$_2$O (**3**). The cation of complex **3** shown in *Fig. 7* has approximate S_4 symmetry, and all four pyrrolidine rings have envelope conformations. Selected bond lengths and angles are given in *Table 3*. In ring N(2), C(6), C(7), C(8),

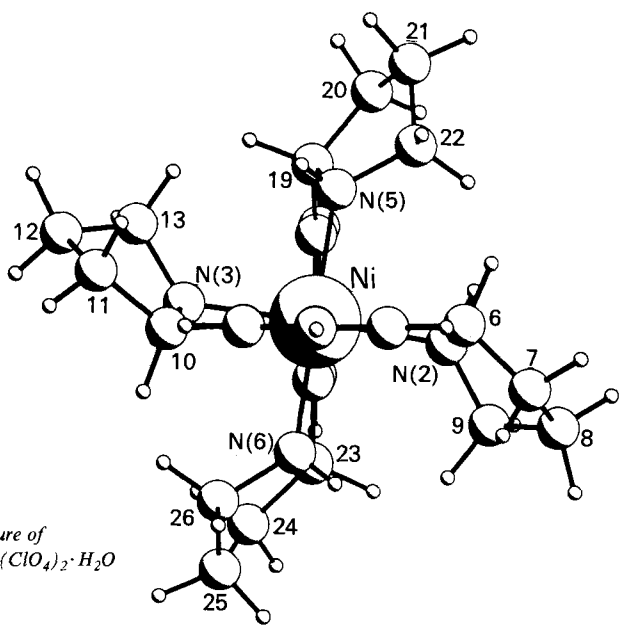

Fig. 7. *X-Ray crystal structure of [Ni{(+)-bpp}{(−)-bpp}](ClO$_4$)$_2$·H$_2$O* (**3**). Arbitrary numbering.

Table 3. *Selected Bond Lengths* [Å] *and Bond Angles* [°] *of [Ni{(+)-bpp}{(−)-bpp}](ClO$_4$)$_2$·H$_2$O* (**3**). Arbitrary numbering.

Ni–N(1)	2.005(5)	N(1)–Ni–N(2)	79.67(22)	N(2)–Ni–N(5)	91.88(18)
Ni–N(2)	2.182(5)	N(1)–Ni–N(3)	79.51(20)	N(2)–Ni–N(6)	91.56(19)
Ni–N(3)	2.173(4)	N(1)–Ni–N(4)	177.74(19)	N(3)–Ni–N(4)	99.95(17)
Ni–N(4)	2.011(5)	N(1)–Ni–N(5)	98.48(19)	N(3)–Ni–N(5)	92.28(17)
Ni–N(5)	2.168(4)	N(1)–Ni–N(6)	102.29(19)	N(3)–Ni–N(6)	91.76(17)
Ni–N(6)	2.198(5)	N(2)–Ni–N(3)	159.16(20)	N(4)–Ni–N(5)	79.34(19)
		N(2)–Ni–N(4)	100.89(20)	N(4)–Ni–N(6)	79.90(19)
				N(5)–Ni–N(6)	159.23(19)

C(9), atom C(8) is displaced by 0.47(2) Å from the best plane through the remaining four atoms (planar within 0.047 Å). Atom C(8) undergoes considerable thermal motion with the result that the bond length and angles in which it is involved are distorted from normal values. In ring N(3), C(10), C(11), C(12), C(13), atom C(12) is displaced by – 0.60(1) Å from the best plane through the remaining four atoms (planar to within 0.049 Å). In ring N(5), C(19), C(20), C(21), C(22), atom C(21) is displaced by 0.63(1) Å from the best plane through the remaining four atoms (planar within 0.058 Å). In ring N(6), C(23), C(24), C(25), C(26), atom C(25) is displaced by 0.64(1) Å from the best plane through the remaining four atoms (planar within 0.025 Å).

4. Discussion. – Stereoselectivity was shown to be absent in the formation of binary complexes with diamines [6] and bidentate natural amino acids [7]. Even for facially coordinating tridentate amino acids, voluminous coordinating groups seem to be required for stereoselectivity: 1:2 complex formation was stereoselective with histidine [4] but not with aspartic and glutamic acid [8] or with 2,3-diaminopropionic acid. On the other hand, stereoselectivity was favoured by the presence of coordinating or non-coordinating substituents on the N-atoms [9].

Compared to known cases – some typical examples of which are given in *Table 4* – the formation of $[Ni(bpp)_2]^{2+}$ is surprisingly selective and shows, to our knowledge, the highest stereoselectivity ever observed for the formation of binary complexes involving labile coordination centers, and this dispite the absence of any secondary binding interactions between the two ligand molecules.

Table 4. *Typical Examples of Stereoselectivity in the Formation of Octahedral 1:2 Metal-to-Ligand Complexes of Nickel(II)*

Ligand	$\log\beta_2(rac)$	$\log\beta_2(meso)$	$\Delta\Delta G$[a])	Ref.
N-(2-hydroxybenzyl)alanine	15.01	14.81	+1.89	[10]
Penicillamine	23.02	22.87	+2.57	[11]
Histidine	15.49	16.15	−2.05	[12]
N-Methylhistidine	15.05	16.10	−4.27	[12]
N,N-Dimethylhistidine	12.13	13.62	−6.78	[12]
3-(Pyrid-2-yl)alanine	15.32	17.45	−3.65	[13]
2,6-Bis(pyrrolidin-2-yl)pyridine	15.27	17.56	−11.33	This work

[a]) Defined as $\Delta\Delta G = -RT(\ln\beta_2(meso) - \ln\beta_2(rac) - \ln 2)$.

Two reasons can be put forward to explain this behaviour. Firstly, the structure of the ligand bpp implies a very rigid arrangement in the coordinated form. The only possible conformational change seems to be restricted to the atoms C(4) and C(4′) of the five-membered rings (**I**). The corresponding CH_2 groups can theoretically oscillate between two positions, which can be designed as '*endo*' and '*exo*' following their positions relative to the coordination center (*Fig. 7*). As can be seen from the X-ray structure of **3**, all four five-membered rings are found in the – apparently more favourable – '*exo*'-configuration in the solid state. In fact, examination of models reveals that in the '*endo*'-configuration, much stronger interactions must occur between the CH_2 H-atoms and the H-atom on the N-atom of the second ligand molecule. In comparison to this fixed conformation, it may

be mentioned that a fluxional behaviour of a pyrrolidine was found in solid cobalt(III) complexes with a similar ligand systems [1].

The strong sterical interactions as a reason for the high stereoselectivity is equally demonstrated by the large difference between the $\log K$ values for the binding of the first and of the second ligand molecule, which is 7.39 and 5.10 log units for the optically active and the *meso*-complex, respectively (see *Table 1*). The difference of the same constants is 1.23 log units only in the case of the Ni^{II} complex with 2,6-bis(aminomethyl)pyridine (bamp), a structurally analogous but sterically more favorable ligand ($\log K_1 = 10.34$; $\log K_2 = 9.11$) [14].

A second reason for the high stereoselectivity may be the C_2 symmetry and the strictly peripheral coordination mode of the ligand bpp which allows only one single arrangement of the two ligand molecules in both the *meso* and the optically active species. Contrary to this, all other examples mentioned in *Table 4* allow two or more different arrangements of the ligand molecules in the racemic as well as in the optically active species. In fact, the relative stability of different isomeric forms can be different for the racemic or the optically active ligand. This can decrease the apparent stereoselectivity which, in labile systems, is the only overall effect between all the forms of the complexes with the ligands of the same and all the forms of the complexes with ligands of opposite chirality. In relation to this, it is interesting to note that the measurements of the stability of mixed ligand complexes of copper(II) with racemic or *meso*-bpp and bidentate amino acids showed no significant stereoselectivity [2]. In fact, in these complexes, one coordination site remains available, and this allows a different coordination mode for the amino acid following the orientation of the substituent.

Compared with Ni^{II}, the 1:2 complex formation of the other bivalent metal ions with (±)-bpp reported in *Table 1* is considerably less stereoselective. The variation of the stereoselectivity for Co^{II}, Ni^{II}, Zn^{II}, and Cd^{II} follows the order of the variation of ionic radii for the corresponding high-spin complexes [15], but the influence of ionic radii on the stereoselectivity is very much higher for bpp than for other ligands, such as histidine [4] or 3-(pyrid-2-yl)alanine [13], for which the similar stereoselectivity series $Co^{II} < Ni^{II} > Zn^{II} > Cu^{II}$ was observed.

The Zn^{II} complex is a special case. The titration curves, for the optically active and the racemic ligand bpp with this metal ion, can only be fitted assuming the successive dissociation of two protons from the 1:1 complex forming successively $[Zn(bpp)OH]^+$ and $[Zn(bpp)(OH)_2]$. The two titration curves are definitely different between 1 and 3 equiv. of NaOH indicating the stereoselectivity of the reaction. On the other hand, the first step of hydrolysis starts at lower pH than the formation of the 1:2 species, and the maximum relative amount of this species formed with the optically active ligand remains small (*ca.* 16% for the conditions of the titration). The precision with which the corresponding formation constant can be determined is, therefore, somewhat lower than for the other metal ions given in *Table 1*.

The authors are very grateful to the *Swiss National Science Foundation* for financial support.

Experimental Part

General. Titrations for Co^{II}, Cu^{II}, Zn^{II}, and Cd^{II} were performed in bidistilled H_2O under N_2. For 1:2 complex formation with Ni^{II}, the equilibrium was reached too slowly for direct titration. Titration curves were, therefore, obtained by preparing series of solns. containing constant amounts of Ni^{II} and of the ligand in a 1:2 ratio, a slight excess of HCl, and increasing amounts of NaOH. The solns., prepared under N_2, were completed to constant volume by addition of H_2O and kept firmly closed in a thermostated bath. pH values were measured until constant values were obtained. Optical rotations: *Perkin-Elmer* polarimeter *M* 240. Circular dichroism: *Jasco* spectropolarimeter *J-500*.

(+)- and (−)-2,6-Bis(pyrrolidin-2-yl)pyridine ((+)- and (−)-bpp, resp.). Solns. of (+)- and (−)-bpp were obtained by extraction with CH_2Cl_2 of strongly basic solns. containing weighed amounts of (+)-bpp[hydrogen (−)-2,3-di-*O,O'*-(4-toluoyl)-L-tartrate]$_2$ or (−)-bpp[hydrogen (+)-2,3-di-*O,O'*-(4-toluoyl)-D-tartrate]$_2$, synthesized as described in [2]. The dried org. layers were evaporated and the oily residue bulb-to-bulb distilled twice. The product was dissolved in a given amount of HCl of exactly known concentration (*ca.* 0.1N) and quantitatively transferred into a volumetric flask. The concentration of the solns. was determined by back titration with NaOH.

Solns. of the racemic ligand (±)-bpp were prepared in the same manner from an alkaline soln. of an equimolar mixture of both diastereoisomeric salts.

The free ligand was recovered from the mixtures used for titrations containing various amounts of different metal ions as follows: excess Na_2H_2edta was added and the neutralized soln. (pH *ca.* 7) passed through an anion exchange column (*Sephadex QAE*, Cl^-). The column was washed with H_2O and the eluent and the washing water concentrated to a small volume. NaOH was added in excess and the ligand isolated by extraction and distillation as described above.

Aqua[(±)-2,6-bis(pyrrolidin-2-yl)pyridine]copper(II) Perchlorate–Water (1/2) ([Cu{(±)-bpp}H_2O]$(ClO_4)_2 \cdot 2H_2O$; **1**). A soln. containing equivalent amounts of $CuSO_4 \cdot 5H_2O$ and (±)-bpp was adsorbed on a chelating ion exchanger (acryl-iminodiacetate). After washing of the column, the complex was eluted with 2N $HClO_4$. After neutralization with 2N NaOH, the complex crystallized as the perchlorate salt. The crystals were filtered, washed with a small amount of cold H_2O, EtOH, and acetone. Successive concentration of the mother liquors gave a total yield of 80%. For X-ray structural analysis, a small sample of **1** was recrystallized from H_2O.

*Tris{[(+)-2,6-bis(pyrrolidin-2-yl)pyridine]copper(II)} Sulfate–Water–[(−)-Di-*O,O*-(4-toluoyl)-L-tartaric Acid] (1/2/1)* ([Cu{(+)-bpp}]$_3(SO_4)_3 \cdot 2H_2O \cdot$(−)-di-*O,O'*-(4-toluoyl)-L-tartaric acid]; **2**). Hot solns. of $CuSO_4 \cdot 5H_2O$ (0.5 g, 2 mmol) in H_2O (10 ml) and of ((+)-H_2bpp)[(−)-di-*O,O'*-(4-toluoyl)-L-tartrate]$_2 \cdot 3/2H_2O$ [2] (2.1 g, 2 mmol) in EtOH (60 ml) and H_2O (10 ml) were mixed and evaporated. The solid was dissolved in EtOH/AcOEt 1:1. On cooling, 0.9 g of a blue crystalline solid was obtained. Recrystallization of 0.3 g of the solid in EtOH (10 ml), AcOEt (10 ml), and H_2O (2 ml) gave a blue powder. To obtain crystals of **2** suitable for X-ray determination, the powder was recrystallized from pure EtOH.

[(+)-2,6-Bis(pyrrolidin-2-yl)pyridine][(−)-2,6-bis(pyrrolidin-2-yl)pyridine]nickel(II) Perchlorate–Water (1/1) ([Ni{(+)-bpp}{(−)-bpp}]$(ClO_4)_2 \cdot H_2O$; **3**). The solns. prepared as indicated above, containing (±)-bpp and $NiSO_4 \cdot 6H_2O$ in a 2:1 ratio, and which were used for the determination of the titration curves, were put together and neutralized with $HClO_4$. On addition of excess $NaClO_4$, **3** crystallized almost quantitatively as small pale violet plates. The complex was recrystallized several times from hot H_2O. Crystals of suitable size for X-ray determination were finally obtained by very slow cooling of warm saturated aq. solns.

X-Ray Structure Determinations. Details of crystal data and refinement are given in *Table 5*. X-Ray analysis of **1**–**3**: Data were collected using a *Stoe-AED2* four-circle diffractometer with graphite monochromated MoK_α radiation. Standard reflections were measured every h. The structures were solved by direct methods or *Patterson-Fourier* methods using the NRCVAX system [16], which was also used for refinement and all further calculations. In **1**, H-atoms were located from difference maps and refined isotropically. In **2** and **3**, the H-atoms were included in calculated positions and held fixed ($U_{iso} = U_{eq} + 0.01$ Å^2). In **3**, the N*H* atoms were located from difference maps but were held fixed during refinement ($U_{iso} = 0.075$ Å^2). The H-atoms of H_2O could not be located in **2** and **3**. The non-H-atoms were refined anisotropically by weighed full-matrix least-squares. However, owing to the limited data available for structure **2**, only the Cu-, S-, and O-atoms were refined anisotropically. Neutral complex-atom scattering factors used in NRCVAX are from [17]. Final positional and equivalent isotropic thermal parameters were deposited with the *Cambridge Crystallographic Data Center*, England. Selected interatomic distances and angles are given in *Tables 2* and *3*. The numbering schemes used are illustrated in *Figs. 5–7*, prepared using the program PLUTO [18]. Structure-factor tables are available from *H. St.-E.*

Table 5. *Crystal Data and Experimental Details*

	1	**2**	**3**
Empirical formula	$C_{13}H_{21}CuN_3O$ $(ClO_4)_2 \cdot 2\,H_2O$	$[C_{13}H_{19}CuN_3]_3$ $(SO_4)_3 \cdot 2\,H_2O \cdot C_{20}H_{18}O_8$	$[C_{13}H_{19}N_3]_2Ni$ $(ClO_4)_2 \cdot H_2O$
M_r	533.8	1553.8	710.23
Crystal colour, habit	blue blocks	blue cubes	voilet plates
Crystal system	monoclinic	orthorhombic	monoclinic
Space group	$C2/c$	$P2_12_12_1$	$P2_1/a$
Z	4	4	4
D_c [g/cm^3]	1.674	1.481	1.512
Linear absorption coefficient μ(MoK_α) [cm^{-1}]	12.9	10.7	8.5
Crystal dimensions [mm]	0.42, 0.27, 0.19	0.20, 0.13, 0.22	0.42, 0.30, 0.23
Cell parameters: least-squares fit of			
No. of reflections	20	17	20
2Θ range [°]	12–30	10–22	28–34
a [Å]	12.484(3)	11.754(2)	17.083(2)
b [Å]	10.788(2)	19.794(2)	11.771(2)
c [Å]	16.668(3)	29.926(4)	17.199(3)
β [°]	109.31(1)		115.58(1)
V [Å^3]	2118.5(7)	6062.5(17)	3119.5(8)
Scan mode	ω/Θ	ω/Θ	ω/Θ
$2\Theta_{max}$ [°]	50	40	50
h,k,l Range	±14, ±12, +19	+11, +19, +28	±20, +13, +20
No. of reference reflections	3	3	2
and variation [%]	1	6	2
No. reflections measured	3743	3646	5510
No. unique reflections	1874	3646	5510
No. of reflections used in refinement	1788	2474	2973
x in $[I > x\sigma(I)]$	2.5	1.5	2.5
No. parameters refined	188	525	397
R	0.036	0.072	0.054
wR	0.077	0.079	0.074
k in $w^{-1} = \sigma^2(F_o) + k(F_o^2)$	0.003	0.003	0.002
max shift/sigma ratio	0.057	0.141	0.030
Residual density:			
max [e/Å^3]	0.28	0.77	0.51
min [e/Å^3]	−0.28	−0.48	−0.32

REFERENCES

[1] K. Bernauer, H. Stoeckli-Evans, D. Hugi-Cleary, H.J. Hilgers, H. Abd El-Khalek, J. Porret, J.-J. Sauvain, *Helv. Chim. Acta* **1992,** *75,* 2327.
[2] K. Bernauer, F. Gretillat, *Helv. Chim. Acta* **1989,** *72,* 477.
[3] K. Bernauer, S. Bourqui, D. Hugi-Cleary, R. Warmuth, *Helv. Chim. Acta* **1992,** *75,* 1388.
[4] P.J. Morris, R.B. Martin, *J. Inorg. Nucl. Chem.* **1970,** *32,* 2891.
[5] H.B. Gray, 'Transition Metal Chemistry', Ed. R.L. Carlin, Vol. 1, 1965, 239.

[6] A. T. Advani, D. S. Barnes, L. D. Pettit, *J. Chem. Soc. A*, **1970**, 2691.
[7] D. S. Pettit, R. J. W. Hefford, 'Metal Ions in Biological Systems', Ed. H. Sigel, Marcel Dekker, New York, 1979, Vol. 9, p. 173, and ref. cit. therein.
[8] J. H. Ritsma, G. A. Wiegers, F. Jellinek, *Recl. Trav. Chem. Pays-Bas* **1965,** *84*, 1577.
[9] V. A. Davankov, R. P. Mitchell, *J. Chem. Soc. Dalton* **1972,** 1012.
[10] J. H. Ritsma, *Recl. Trav. Chim. Pays-Bas* **1975,** *94*, 174.
[11] J. H. Ritsma, F. Jellinek, *Recl. Trav. Chim. Pays-Bas* **1972,** *91*, 923.
[12] J. H. Ritsma, *J. Inorg. Nucl. Chem.* **1976,** *38*, 907.
[13] P. R. Rechani, R. Nakon, R. J. Angelici, *Bioinorg. Chem.* **1976,** *5*, 329.
[14] M. Ferigo, Thèse, Neuchâtel, 1988.
[15] R. D. Shannon, *Acta Crystallogr. Sect. A* **1976,** *32*, 751.
[16] E. J. Gabe, Y. Le Page, J.-P. Charland, F. L. Lee, P. S. White, *J. Appl. Crystallogr.* **1989,** *22*, 384.
[17] 'International Tables for X-Ray Crystallography (1974)', Vol. IV, Birmingham, Kynoch Press (present distributor, Kluwer Academic Publishers, Dordrecht).
[18] W. D. S. Motherwell, W. Clegg, 'PLUTO, Programm for Plotting Molecular and Crystal Structures (1978)', University of Cambridge, England.